J Neurol (2006)
DOI 10.1007/s00415-006-0164-5

ORIGINAL COMMUNICATION

Christian Enzinger
Stephen Smith
Franz Fazekas
Gunther Drevin
Stefan Ropele
Thomas Nichols
Timothy Behrens
Reinhold Schmidt
Paul M. Matthews

# Lesion probability maps of white matter hyperintensities in elderly individuals

## Results of the Austrian stroke prevention study

Received: 30 June 2005
Received in revised form: 31 October 2005
Accepted: 7 November 2005
Published online: 10 April 2006

C. Enzinger, MD (✉) · F. Fazekas, MD
S. Ropele, PhD · R. Schmidt, MD
Department of Neurology
Medical University Graz
Auenbruggerplatz 22
8036 Graz, Austria
Tel.: +43-316/385/2981
Fax: +43-316/325520
E-Mail: chris.enzinger@meduni-graz.at

F. Fazekas, MD · C. Enzinger, MD
Division of Neuroradiology
Department of Radiology
Medical University Graz, Austria

S. Ropele, PhD
MR Research Unit
Medical University Graz, Austria

S. Smith, Dphil · T. Behrens, Dphil
P. M Matthews, MD, DPhil, FRCP
C. Enzinger, MD
The Centre for Functional MRI of the Brain
John Radcliffe Hospital
University of Oxford, UK

G. Drevin, PhD
The School for Computer,
Statistical and Mathematical Sciences
Potchefstroom University for CHE
South Africa and School of Computing
Science
Riddlesex University
United Kingdom

T. Nichols, PhD
The Department of Biostatistics
University of Michigan, USA

**Abstract** *Objective* White matter hyperintensities (WMH) are common on brain MRI of the elderly. Their size ranges from punctate to early confluent to confluent lesions. While this increase in extension is frequently seen as evidence for a continuum of changes, histological data and clinical follow-up suggest differences in underlying pathology and their progression. *Methods* We tested this hypothesis by exploring the distributions of punctuate and confluent lesions using lesion probability maps (LPM) generated from MRI scans of 189 participants (mean age 60.8+/−6.2 years) in the Austrian Stroke Prevention Study. We dichotomised WMH according to the classification by Fazekas et al. [punctate (n=143) vs. early confluent and confluent (n=33)] to run voxel-based t-tests using permutation-based nonparametric inference. To test alternative hypotheses, we created similar LPM for age and arterial hypertension. *Results* We observed significant differences in the spatial distribution of lesions for the two WMH groups ($p<0.01$). Punctate lesions were more diffusely distributed throughout the cerebral white matter (peak probability ~5%) relative to confluent lesions (peak probability 45%). Confluent lesions had greatest likelihood of being found in perfusion "watershed" regions. These differences in distribution could not be explained by differences in age or hypertension only, as both greater age and the diagnosis of hypertension were associated with WMH abutting the occipital horns. *Conclusions* Punctate and early confluent to confluent WMH show distinguishable differences in their spatial distribution within a normal elderly population. The pattern of punctate WMH is probably a consequence of mixed etiologies. Preferential localization of the more confluent WMH with arterial watershed areas implies a stronger ischemic component in their development.

**Key words** ageing · probability maps · white matter hyperintensities · white matter lesions · cerebral small vessel disease

## Introduction

White matter hyperintensities (WMH) are a frequent finding on MRI of the brain in elderly individuals [1]. They are commonly viewed as a neuropathological continuum from punctate to confluent abnormalities. However, there are indications that they may – to a certain extent - represent etiologically different entities

[1–5]. Further clarification of the genesis of WMH is necessary if they are to be used as a surrogate marker for small vessel disease in future clinical trials [6].

While important, the potential role of histopathology in elucidating the etiology of WMH is limited. There is only limited material with which to study the histopathological correlates of WMH [2, 7, 8] and when appropriate material is available, it is difficult to precisely co-localise small lesions on MRI and changes in histopathological sections. Also, a strong reporting bias towards uncommon etiologies of WMH must be anticipated in correlative histopathological investigations.

Complementary information, less biased towards extremes of pathology, can come from lesion probability maps (LPM) generated from MRI of living populations. LPM have proven to be a powerful tool for the in vivo study of lesion distributions in other white matter disorders [9–11]. LPM have also been used to characterise imaging changes in ageing cohorts both without [12] and with variable degrees of cognitive impairment [13]. Defining the distribution of lesions in white matter can potentially provide indirect clues regarding the mechanisms of lesion development.

Here, we wished to test whether WMH with different MRI appearance demonstrate different patterns of spatial distributions by generating separate LPM of different lesion grades from images for a large cohort of elderly, community-dwelling subjects without known neurological or psychiatric disease. As both the frequency and the extent of WMH appear to increase with age and hypertension [1, 14–17], we generated similar LPM dichotomized for age and the diagnosis of hypertension to evaluate the independent effects of these factors on WMH distribution.

## Materials and methods

### Study cohort

MRI scans of a subset of 189 participants (95 females and 94 males, mean age 60.8+/−6.2 years) in the Austrian Stroke Prevention Study (ASPS) which had been obtained at the time of risk-factor assessment at the baseline of this study were used to generate lesion probability maps as described below. The ASPS is a prospective single-centre study in community-dwelling volunteers aged 50–75 years without neuropsychiatric disease (for details concerning design, definition of risk factors and medical conditions see [18]. Here, arterial hypertension was defined as a history of arterial hypertension with repeated blood pressure readings of ≥140/90 mm Hg, if the readings at the examination exceeded these limits or if a subject was on antihypertensive medication [19]. Arterial hypertension was present in 99 subjects (52.4%) and 46 of those received antihypertensive medication. The study was approved by the local ethics committee. All participants gave written informed consent. The subject demographics of the entire study cohort and for subgroups according to WMH grade at baseline are presented in the Table 1.

### MRI of the brain

MRI of the brain was performed on 1.5 T scanners of the same manufacturer (Philips Medical Systems; Eindhoven, the Netherlands). We obtained axial $T_2$- and proton-density weighted images (repetition time 2000 to 2500 ms; echo time 30 and 60 ms) and sagittal $T_1$-weighted images (repetition time/echo time = 600/30 ms). Slice thickness was 5 mm and matrix size was 256×256 pixels.

### Identification, rating and segmentation of WMH

Blinded to clinical information, CE identified white matter lesions comparing signal characteristics on all sequences, drew their outlines onto a transparency overlaid on hard-copies of proton-density weighted images, and graded the lesions in each brain scan according to the scheme of Fazekas et al. [20] as absent (n=13), punctate (n=143), early confluent (n=22), and confluent (n=11).

**Table 1** Subject demographics of the entire study population and for subgroups according to WMH grade at baseline

| | Entire cohort (n=189) | WMH grade 1 (n=143) | WMH grade 2 or 3 (n=33) | p |
|---|---|---|---|---|
| Age, years | 60.8±6.2 | 59.9±5.9 | 65.1±5.4 | 0.001 |
| Gender (female/male) | 95/94 | 76/67 | 14/19 | 0.26 |
| Diabetes, n, % | 9 (4.8%) | 6 (4.3%) | 3 (9.1%) | 0.37 |
| Arterial hypertension, n, % | 99 (52.4%) | 73 (51.0%) | 19 (57.6%) | 0.49 |
| Antihypertensive drugs, n, % | 46 (24.3%) | 32 (22.4%) | 13 (39.4%) | 0.04 |
| Cardiac disease, n, % | 65 (34.4%) | 49 (34.3%) | 12 (36.4%) | 0.84 |
| Current smokers, n, % | 16 (8.5%) | 14 (9.2%) | 1 (3.0%) | 0.20 |
| Body Mass Index (kg/m$^2$) | 26.8±3.7 | 26.7±3.7 | 26.9±3.2 | 0.77 |
| Systolic BP, mmHg | 138.2±20.4 | 137.1±20.8 | 145.0±18.6 | 0.05 |
| Diastolic BP, mm Hg | 85.1±9.0 | 85.5±9.4 | 86.0±8.7 | 0.75 |
| Cholesterol, mg/dl | 227.3±38.9 | 230.3±39.0 | 221.4±40.2 | 0.24 |
| Triglycerides, mg/dl | 142.6±78.1 | 144.3±76.7 | 142.0±91.4 | 0.88 |
| Fibrinogen, mg/dl | 309.6±77.3 | 307.6±78.0 | 308.7±71.7 | 0.93 |
| HbA1c, % | 5.7±0.8 | 5.7±0.8 | 5.9±1.1 | 0.43 |
| Fasting glucose, mg/dl | 94.6±21.5 | 94.9±20.7 | 95.6±28.4 | 0.87 |

BP = blood pressure. WMH = white matter hyperintensities. WMH grades 1, 2, and 3 = punctate, early confluent, and confluent lesions, respectively. Subgroups according to WMH grade compared using Chi-square test, unpaired Student's t-test and Mann-Whitney U-test

Symmetrical hyperintense "caps" around the frontal horns and the appearance of a regular periventricular lining were disregarded as they have been shown to represent normal anatomical variants [2]. Signal alterations in the basal ganglia and pons also were disregarded. Particular attention was paid to avoid misclassification in case of Virchow-Robin spaces or lacunes [21]. Using these templates, lesion mask images were then created independently from the visual rating by a trained technician on proton-density weighted images with the DISPImage programme (Plummer DL, 1992) [22].

### Lesion probability maps (LPM)

The original proton density-weighted images were registered to the Montreal Neurological Institute (MNI152) standard space image using affine registration with FLIRT (FMRIB's Linear Image Registration Tool) [23]. The resulting transforms were then applied to the lesion mask images to put these into standard space. All registrations were checked visually to ensure there was no gross failures of alignment. Lesion mask images in standard space were binarised (i.e. all segmented voxels within the traced regions of interest were considered).

Voxelwise statistics were then carried out to give lesion probability maps at each standard space voxel. Within these maps, the probability of finding a lesion in any given voxel is defined by the relative voxel intensity. Modelling and inference using standard general linear model design set-up was accomplished using permutation-based cluster analysis [24] as implemented in FMRIB's Software Library (FSL) [26].

Permutation-based nonparametric inference (similar to the bootstrap approach) is used for inference on statistic maps when the null distribution is not known [24]. This enables one to carry out accurate inference (i.e., thresholding correctly at a given probability level) for cases where the data and/or pre-thresholding analysis methodology used does not allow simple direct approaches (such as turning true t-values directly into p-values). 5000 permutations were randomly generated when building up the null-distribution to test against.

We characterised the spatial deployment of white matter lesions in various groups at two levels. First, we used lesion probability maps by combining the lesion segments over subjects. These are reported descriptively to quantify the spatial profile of lesion occurrence in each group. Second, we tested for regionally specific differences in the expression of lesions among different groups using voxel-based morphometry. This involved comparison of the mean lesion load at each voxel from two groups using non-parametric techniques. We compared subjects with punctuate lesions (WMH grade 1; n=143) and subjects with early confluent and confluent lesions (WMH grades 2 and 3; n=33). In addition, we compared young and old subjects (dichotomised by the median = 61 years) and subjects with and without a diagnosis of arterial hypertension (n = 99 and 90) to show that differences between punctate and early confluent / confluent lesions exhibit a distinct and regionally specific effect that may be etiologically important.

Clusters were formed according to a defined threshold and corrected for multiple comparisons (across space) within the permutation framework by building up the null distribution of the maximum cluster size (for each permutation). Multi-scale smoothing was applied (0, 1.5, 2, and 4 mm WHM) in order to allow smoothing to match signal [25] with appropriate correction for multiple comparisons. This scale-space search or multi-smoothing component is a very important part of our analysis. The size of the smoothing kernel determines the scale at which inferences about the differences in regional lesion-load are expressed. This can be seen by noting that, after smoothing, the lesion maps correspond to a weighted average lesion-load in the area under the smoothing kernel or filter. A scale-search space, of the sort that we have employed, involves testing for differences at each point in the brain and at a series of different smoothnesses. From the raw timage, at each spatial smoothing scale, clusters were defined and each cluster is size was converted into a p value through the use of the permutation testing (i.e. testing against the null distribution of maximum cluster size over space, and hence fully correcting for multiple comparisons). The optimal p over different scales was then kept.

### General statistical analyses

The Statistical Package of Social Sciences (PC+; version 11.5; SPSS Inc., Chicago, IL) was used to test categorical variables by Pearson's chi-square test and continuous variables by Student's t-test or the Mann-Whitney U test, where appropriate. The level of significance was set at 0.05.

## Results

We observed typical distributions of WMH in the cerebral white matter, with lesion clusters around the anterior and posterior horns of the lateral ventricles and in the centrum semiovale. The Fig. 1**a** and 1**b** show maps of the sample proportion of patients with a WMH at that voxel in standard space (generating lesion probability maps or LPM), with subjects grouped according to lesion classifications (i.e. WMH grades) on the individual scans. In these LPM representations, the voxel intensity characterises the probability of finding a lesion in that voxel across the study population (the color bar denotes the probability).

Lesions were localised more consistently in patients with confluent lesions. The maximum local probability for lesions in subjects with WMH scores 2 and 3 was almost ten times higher (peak probability: 45%; Fig. 1b) than in subjects with WMH score 1 (peak probability ~5%, Fig. 1a). A two-sample t test comparing the proportion of WMH at each voxel between the two groups identified specific white matter areas to be significantly more frequently involved in subjects with early confluent and confluent relative to the punctate lesions (significant clusters, $p<0.01$ corrected; Figs. 1c and 1d). These areas corresponded anatomically to the watershed zones between the vascular territories of the middle cerebral artery, the perforators from the internal carotid and basilar arteries, and the anterior cerebral artery.

To test if these differences could simply be explained by two factors which have been reported previously to increase both frequency and extent of WMH, we generated similar images of t-statistics dichotomising by age and hypertension. Although there was a greater abundance of WMH in older individuals, differences in distribution between older (mean age 66.1±3.7 years) and younger patients (mean age 55.9±3.5 years) were only significant for comparatively small white matter areas abutting the posterior

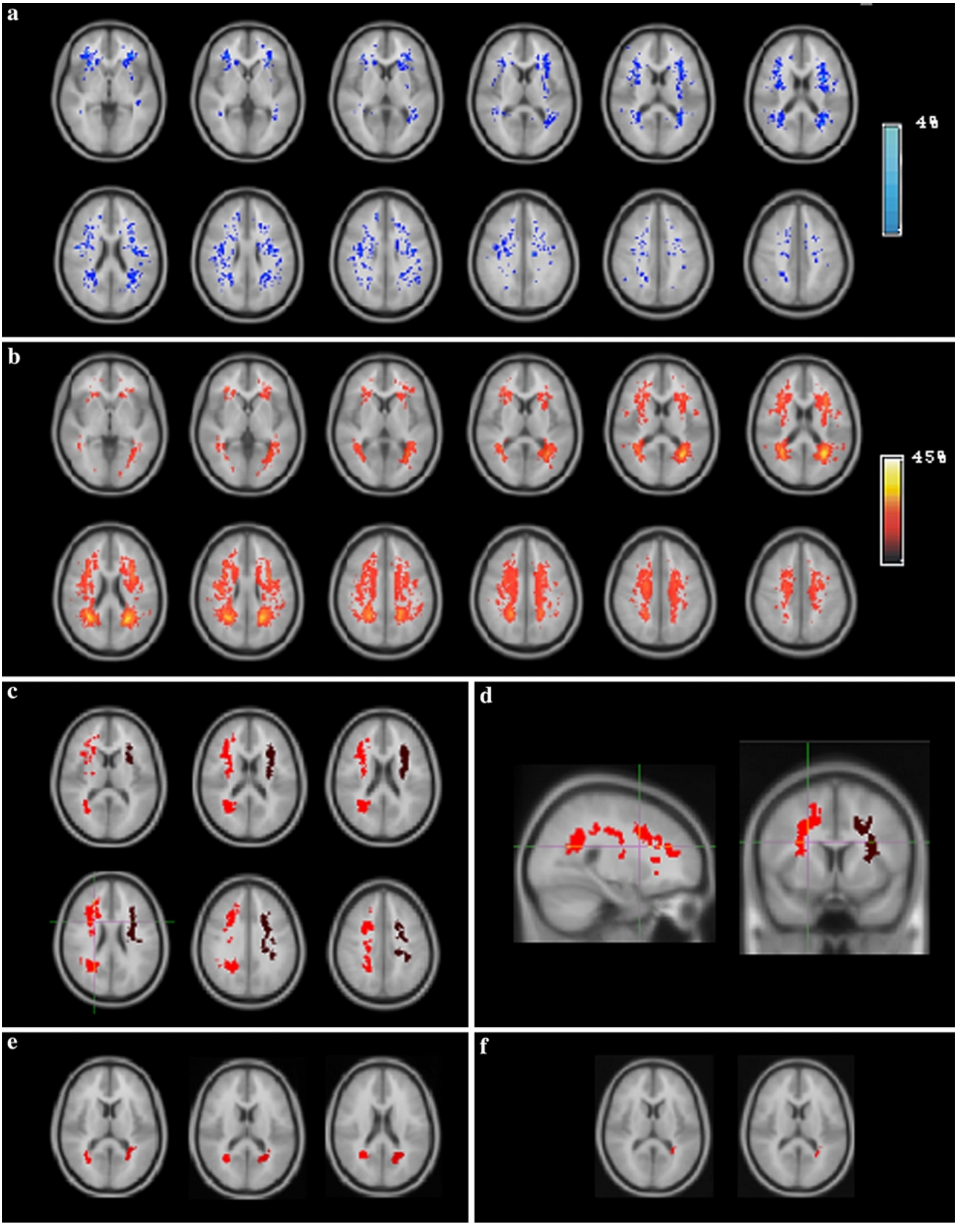
a
48
b
458
c
d
e
f

◀

**Fig. 1 White matter lesion grade, age, arterial hypertension and spatial distribution of lesions. (a, b)** Maps of the sample proportion of patients with a WMH at a given voxel in standard space for punctate lesions (**a**: blue overlays) and early confluent to confluent lesions (**b**: red overlays). Early confluent and confluent WMH are distributed in a more consistent pattern (45% peak probability) compared to the more diffuse distribution of punctate lesions (5% peak probability). The color bar denotes the probability. (**c**) Images of t statistics show significant differences between the spatial distribution of punctate and confluent lesions for frontal white matter areas, lesions in paraventricular location and within the centrum semiovale (significant clusters, $p<0.01$ corrected). (**d**) Sagittal and coronal views of this t-statistics map (defined by the cross-hair shown) illustrate the preferential localisation of more confluent lesions in watershed regions. (**e, f**) White matter areas abutting the posterior horns of the lateral ventricles are significantly more likely to be involved in older than in younger individuals (**e**) and in hypertensive compared to normotensive subjects (**f**; significant clusters, $p<0.01$ corrected)

horns of the lateral ventricles (significant clusters, $p<0.01$ corrected; Fig. 1e).

Only small differences in a similar distribution were found between WMH LPM generated from subjects with a diagnosis of arterial hypertension (mean blood pressure 152.3+/−17.7 to 91.8+/−7.7 mmHg) and subjects without a diagnosis of arterial hypertension (mean blood pressure 123.3+/−9.5 to 78.6+/−4.3 mmHg) (significant clusters, $p<0.01$ corrected; Fig. 1f). Thus, the factors age and hypertension did not explain the differences in lesion patterns found for the different groups defined by WMH grade (Figs. 1c and 1d).

## Discussion

Using lesion probability maps which directly represent consistent image changes across groups of subjects, we have been able to confirm the distribution pattern of WMH reported by expert readers on the basis of observations of individual subject scans [21].

The spatial distribution of WMH in our study cohort also closely resembles the patterns of WMH distribution recently observed by other groups using similar mapping techniques [12, 13]. In addition, we dichotomised LPM on the basis of lesion appearances to check for differences in lesion distributions with low and high lesion loads and found significant differences. Punctate WMH were observed in a more diffusely scattered pattern, reflected by a low local peak probability. In contrast, early confluent and confluent WMH followed a more consistent pattern. A direct contrast between the two groups showed that lesions were significantly more frequently found in arterial watershed regions in subjects with early confluent and confluent white matter disease. Interestingly, there also was only incomplete overlap between individual lesions in subjects with punctate WMH and those with confluent WMH.

If punctate and confluent lesions exclusively represent the result of a common process with confluent lesions evolving from punctate changes, then exactly identical lesion distributions would be expected. On the basis of this cross-sectional "snap-shot" of lesion distributions with different lesion appearances, it appears that this is only true for a specific subset of punctate lesions, i.e. those that are located in the white matter abutting the occipital horns of the ventricles and within watershed regions of the centrum semiovale. These punctate lesions might therefore represent "crystallisation points" for confluence of lesions.

For the remainder of punctate lesions, no direct association with subsequent confluency can be assumed which would appear to indicate etiological heterogeneity of punctate WMH in this older population. A difference in etiology also is suggested by an earlier correlative imaging and histopathological study [2] which provided evidence that punctate WMH correspond to a range of minor pathological changes of predominantly non-ischemic origin, while larger, confluent WMH have an identifiable ischemic component. Consistent with this, longitudinal observations show substantial progression of lesions only in subjects with confluent WMH at baseline [3]. Different relations between cardiovascular risk factors and worsening of WMH with different WMH grades at baseline have also been reported by others [27].

As demonstrated previously [14–17], we also found more frequent WMH with ageing and hypertension. However, in our study, these factors appeared to be weaker independent determinants compared with the rated WMH score and changes were confined to white matter regions abutting the posterior horns of the lateral ventricle. A visual check for periventricular areas of relative atrophy made sure that reported lesion density changes did not fall close to the atrophy change regions. Because our study participants were "healthy" community-dwelling subjects and a high proportion of these were on antihypertensive treatment, possible differences with these contrasts may have been reduced. The methodological impossibility of isolating single risk factors and also the interactions between commonly co-expressed traits also may have obscured potential differences. Nonetheless, the factors age and hypertension do not appear to have contributed significantly to the differences in lesion distributions found between different WMH grades.

Caveats that need to be considered when interpreting our results include that the contrast created between subjects according to WMH grade was based on unequal and (in the case of subjects with confluent lesions) relatively low numbers of subjects. This limited sample of subjects with more severe white matter damage could have influenced our results.

A lower sample size could translate to less probability for variance within a group relative to the bigger sample of subjects with punctate lesions. However, one of the advantages of permutation methods lies in their applicability even when the assumptions of a parametric approach are untenable [24]. Also, by definition, WMH grades 2 and 3 comprise larger lesions, which might have affected the estimation of lesion probabilities. Intuitively, as more widespread (i.e., confluent) lesions tend to occupy a larger number of voxels, an intrinsically higher likelihood for overlap between subjects in individual voxels must be expected. It is not inconceivable that this relationship might be a major determinant of the differences observed in the t-tests between groups. Also, different vascular mechanisms (such as atherosclerosis and microangiopathy) might have contributed to differences in WMH patterns. However, in this study population of normal elderly volunteers, the frequency of hemodynamically significant carotid stenosis is below 5%, which clearly limits a possible pathogenetic impact or modulation of the effect of risk factors. Similarly, the overall prevalence of diabetes in our cohort is low (4.8%). Unfortunately, the present dataset therefore does not allow testing such hypotheses. Further, it needs to be noted that regular caps around the frontal horns, ventricular linings, bands or halos abutting the ventricles deliberately have not been considered in our analyses, as they have been shown to represent anatomical variants [2]. Also, we did not include signal changes in the pons or basal ganglia in our analyses.

In summary, this study extends previous neuropathological and imaging data [2, 3] to provide new evidence that confluent white matter lesions evolve from only a portion of punctate abnormalities, most likely because the latter are heterogeneous in etiology. Our findings strongly suggest a pathological pattern of confluent WMH associated with clustering around watershed regions, consistent with effects of chronic hypoperfusion. As these confluent lesions appear to have a prominent ischemic component, we suggest that future interventional trials to limit cerebral small-vessel disease [6] should focus on patient subgroups defined by these WMH grades.

**Acknowledgments and Funding** This work has been supported by the FWF Austrian Science Fund (Vienna; CE and SR, grant number J2373-B02 and P15158, respectively), the UK Medical Research Council (PMM) and an EPSRC Advanced Research Fellowship (SS). We also thank all study participants for their enthusiasm with this project. There are no possible conflicts of interest.

## References

1. de Leeuw FE, de Groot JC, Achten E, et al. (2001) Prevalence of cerebral white matter lesions in elderly people: a population based magnetic resonance imaging study. The Rotterdam Scan Study. J Neurol Neurosurg Psychiatry 70:9–14
2. Fazekas F, Kleinert R, Offenbacher H, et al. (1993) Pathologic correlates of incidental MRI white matter signal hyperintensities. Neurology 43:1683–1689
3. Schmidt R, Enzinger C, Ropele S, Schmidt H, Fazekas F, the Austrian Stroke Prevention Study (2003) Progression of cerebral white matter lesions: 6-year results of the Austrian Stroke Prevention Study. Lancet 14:2046–2048
4. Pantoni L (2002) Pathophysiology of Age-Related Cerebral White Matter Changes. Cerebrovasc Dis 13:7–10
5. De Groot JC, De Leeuw FE, Oudkerk M, et al. (2002) Periventricular cerebral white matter lesions predict rate of cognitive decline. Ann Neurol 52:335–341
6. Schmidt R, Scheltens P, Erkinjuntti T, et al. (2004) White matter lesion progression: A surrogate endpoint for trials in cerebral small-vessel disease. Neurology 63:139–144
7. Awad IA, Johnson PC, Spetzler RF, Hodak JA (1986) Incidental subcortical lesions identified on magnetic resonance imaging in the elderly II. Postmortem pathological correlations. Stroke 17:1090–1097
8. Scheltens P, Barkhof F, Leys D, Wolters EC, Ravid R, Kamphorst W (1995) Histopathologic correlates of white matter changes on MRI in Alzheimer's disease and normal aging. Neurology 45:883–888
9. Narayanan S, Fu L, Pioro E, et al. (1997) Imaging of axonal damage in multiple sclerosis: spatial distribution of magnetic resonance imaging lesions. Ann Neurol 41:385–391
10. Lee MA, Smith S, Palace J, et al. (1999) Spatial mapping of T2 and gadolinium-enhancing T1 lesion volumes in multiple sclerosis: evidence for distinct mechanisms of lesion genesis? Brain 122:1261–1270
11. Charil A, Zijdenbos AP, Taylor J, et al. (2003) Statistical mapping analysis of lesion location and neurological disability in multiple sclerosis: application to 452 patient data sets. NeuroImage 19:532–544
12. Wen W, Sachdev P (2004) The topography of white matter hyperintensities on brain MRI in healthy 60- to 64-year-old individuals. NeuroImage 22:144–154
13. DeCarli C, Fletcher E, Ramey V, Harvey D, Jagust W (2005) Anatomical mapping of white matter hyperintensities (WMH). Exploring the relationships between periventricular WMH, deep WMH, and total WMH burden. Stroke 36:50–55
14. Fazekas F, Niederkorn K, Schmidt R, et al. (1988) White matter signal abnormalities in normal individuals: correlation with carotid ultrasonography, cerebral blood flow measurements, and cerebrovascular risk factors Stroke 19:1285–1288
15. de Leeuw F-E, de Groot JC, Oudkerk M, et al. (2002) Hypertension and cerebral white matter lesions in a prospective cohort study. Brain 125:765–772
16. Strassburger TL, Hing-Chung L, Daly EM, et al. (1997) Interactive effects of age and hypertension on volumes of brain structures. Stroke 28:1410–1417

17. Carmelli D, Swan GE, Reed T, Wolf PA, Miller BL, DeCarli C (1999) Midlife cardiovascular risk factors and brain morphology in identical older male twins. Neurology 52:1114–1115
18. Schmidt R, Fazekas F, Kapeller P, Schmidt H, Hartung HP (1999) MRI white matter hyperintensities: three-year follow-up of the Austrian Stroke Prevention Study. Neurology 53:132–139
19. 1999 World Health Organization-International Society of Hypertension Guidelines for the Management of Hypertension. Guidelines Subcommittee. J Hypertens 17:151–183
20. Fazekas F, Chawluk JB, Alavi A, Hurtig HI, Zimmerman RA (1987) MR signal abnormalities at 1.5 T in Alzheimer's dementia and normal aging. Am J Roentgenol 49:351–356
21. Barkhof F, Scheltens P (2002) Imaging of White Matter Lesions. Cerebrovasc Dis 13:21–30
22. Plummer D (1992) DispImage: a display and analysis tool for medical images. Rev Neuroradiol 5:489–495
23. Jenkinson M, Bannister P, Brady M, Smith S (2002) Improved Optimization for the Robust and Accurate Linear Registration and Motion Correction of Brain Images. NeuroImage 17:825–841
24. Nichols TE, Holmes AP (2002) Nonparametric permutation tests for functional neuroimaging: a primer with examples. Hum Brain Mapp 15:1–25
25. Worsley KJ, Marrett S, Neelin P, Evans AC (1996) Searching scale space for activation in PET images. Hum Brain Mapping 4:74–90
26. Smith SM, Jenkinson M, Woolrich MW, et al. (2004) Advances in functional and structural MR image analysis and implementation as FSL. NeuroImage 23:208–219
27. Longstreth Jr WT, Arnold AM, Beauchamp NJ, et al. (2005) Incidence, manifestations, and predictors of worsening white matter on serial cranial magnetic resonance imaging in the elderly. The Cardiovascular Health Study. Stroke 36:56–61